

# Classification of Low and High Schizotypy Levels via Evaluation of Brain Connectivity

**Ahmad Zandbagleh**

*School of Electrical Engineering, Iran University of Science and Technology, Tehran, Iran  
E-mail: a\_zandbagleh@elec.iust.ac.ir*

**Sattar Mirzakuchaki\***

*School of Electrical Engineering, Iran University of Science and Technology, Tehran, Iran  
E-mail: m\_kuchaki@iust.ac.ir*

**Mohammad Reza Daliri**

*School of Electrical Engineering, Iran University of Science and Technology, Tehran, Iran  
E-mail: daliri@iust.ac.ir*

**Preethi Premkumar**

*Division of Psychology, School of Applied Sciences, London Southbank University, London, UK  
E-mail: premkump@lsbu.ac.uk*

**Saeid Sanei**

*School of Science and Technology, Nottingham Trent University, Clifton Lane, Nottingham, UK  
E-mail: saeid.sanei@ntu.ac.uk*

Schizotypy is a latent cluster of personality traits that denote a vulnerability for schizophrenia or a type of spectrum disorder. The aim of the study is to investigate parametric effective brain connectivity features for classifying high versus low schizotypy status. Electroencephalography (EEG) signals are recorded from 13 high schizotypy and 11 low schizotypy participants during an emotional auditory odd-ball task. The brain connectivity signals for machine learning are taken after the settlement of event-related potentials. A multivariate autoregressive (MVAR)-based connectivity measure is estimated from the EEG signals using the directed transfer functions (DTFs) method. The values of DTF power in five standard frequency bands are used as features. The support vector machines (SVM) revealed significant differences between high and low schizotypy. The accuracy, specificity, and sensitivity of the results using SVM are as high as 89.21%, 90.3%, and 88.2%, respectively. Our results demonstrate that the effective brain connectivity in prefrontal/parietal and prefrontal/frontal brain regions considerably changes according to schizotypal status. These findings prove that the brain connectivity indices offer valuable biomarkers for detecting the schizotypal personality. Further monitoring of the changes in DTF following the diagnosis of schizotypy may lead to early identification of schizophrenia and other spectrum disorders.

*Keywords:* Classification, EEG, Effective Brain Connectivity, Electroencephalography, Schizotypal Personality, Schizotypy.

## 1. Introduction

Schizotypy is a dominating model of the putative risk for, and prediction of, subsequent schizophrenia and some spectrum disorders.<sup>1,2</sup> Schizotypy is based on the

continuum between non-clinical psychosis-like experiences and clinical psychotic symptoms, but also multidimensional neurodevelopmental models of the

---

\* corresponding author

brain.<sup>1,3</sup> This multidimensional personality construct comprises many clinical symptoms and non-clinical manifestations.<sup>4,6</sup> Converging pieces of evidence demonstrate that the schizotypal construct has three main dimensions, namely positive, negative and disorganized.<sup>4,7</sup> The composition of these traits varies between psychometric measures of schizotypal personality, specifically with regards to the conceptualization of disorganisation. The Schizotypal Personality Questionnaire (SPQ) is based on the diagnostic criteria of schizotypal personality disorder and formed the selection criteria for the present study.<sup>7,8</sup> Here, positive schizotypy (cognitive-perceptual) includes magical thinking, unusual perceptual experiences, and paranoid ideation. Negative schizotypy (interpersonal) involves social anhedonia or impairment in emotional and social functioning. The disorganized scale describes eccentric behavior or odd speech.<sup>9,10</sup> Empirical and neuroimaging evidences show that alteration in brain functions characterises these schizotypal traits, and these alterations are linked to sensory modalities (perception), attention, working memory, mental imagery, language production, and control of movements.<sup>9</sup> Therefore, understanding how schizotypal traits manifest through the brain function can improve early identification of schizophrenia.<sup>11,12</sup>

The development of non-invasive, low-cost electroencephalography (EEG) tools has paved the way for better study of brain functions.<sup>13</sup> Furthermore, EEG has been used to design machine learning tools for diagnosing psychiatric disorders in recent years.<sup>14</sup> Recent research has examined the EEG signals of individuals with high schizotypy (HS) in resting state<sup>15-19</sup> and during emotion and attention tasks.<sup>20-24</sup> Fuggetta et al.<sup>15</sup> focused on power spectra of different EEG frequency bands and showed that HS participants elicited increased regional alpha oscillations. This abnormality suggested high-level attention in the HS group.

In addition, reduced asymmetry in some frequency bands<sup>16</sup> and frontal alpha asymmetry<sup>17</sup> have been observed in HS individuals during rest. In particular, Yu et al.<sup>16</sup> reported that the extreme level of positive schizotypy has a significant decrease in the frontal and occipital connectivities, especially in alpha frequency that plays a major part in selective information processing<sup>25</sup>. According to the disconnection hypothesis of schizophrenia, Hu et al.<sup>18</sup> showed abnormalities in functional connectivity of alpha activity for two

contrasting schizotypal traits, namely positive and negative, by means of the phase lag index (PLI). Furthermore, studies have tried to evaluate task-related EEGs. Based on Oestreich et al.<sup>20</sup>, non-clinical HS individuals fail to suppress the N1 auditory evoked potential while listening to self-generated speech, a response style that is similar to those of schizophrenia patients. One study<sup>21</sup> suggested that diminished frontal theta and occipital alpha powers while listening to criticism and praise covary with perceived lack of emotional support in HS individuals. These diminished EEG signals correspond to less emotional arousal and more consciousness of emotional information, respectively. A more recent study<sup>22</sup> found abnormalities in both go and stop trials during a stop-signal task at behavioral and neural levels (increased N1 in all stop trials and increased P3 amplitude in 17% of stop trials in HS individuals).

Recently, some studies used machine learning approaches for predicting HS individuals. Jeong et al.<sup>23</sup> used an audiovisual emotion perception task with spatio-temporal event related potential (ERP) features to distinguish between HS and healthy groups by using shrinkage linear discriminant algorithm (SKLDA). They achieved zero false-positive rates in their classification method. Machine learning can also adopt functional connectivity measures. Trajkovic et al.<sup>19</sup> suggested that HS individuals have reduced connectivity in the right frontoparietal brain region in the alpha frequency band. Using a simple classifier, they reached a classification accuracy of 74.3% in two-class problems. Another study<sup>24</sup> examined the abnormalities of auditory sensory gating in three groups (first-episode schizophrenia patients, ultra-high-risk individuals, and healthy people) using functional connectivity and a decision tree classifier. First-episode schizophrenia patients had stronger brain connectivity between the right superior frontal gyrus and right insula than healthy individuals. Moreover, the ultra-high-risk group had higher brain connectivity between the paracentral lobule and the middle temporal gyrus than the healthy individuals. A combination of demographic characteristics, connectivity, cognitive task performance and P50 auditory evoked potential classified the three groups with 79% accuracy.

Although there is evidence of abnormal connectivity in schizophrenia patients<sup>26</sup>, the presence of these abnormalities in the subclinical population of HS

individuals is still unclear. Furthermore, little is known about the behavior of effective brain connectivity in the schizotypy groups, and hardly any EEG connectivity-based approach with sufficient accuracy can be found for this psychotic experience in the literature.

In the present study, we aim to determine the directed transfer functions (DTF) derived from multivariate autoregressive (MVAR) coefficients, as the model-based estimation of brain connectivity. DTF can determine the directionality between different electrodes or brain regions. Therefore, the primary purpose of this study is to distinguish between HS and low schizotypy (LS) states by evaluating the parametric connectivity features. It is hypothesized that reduced DTF between prefrontal/frontal regions and parieto-occipital regions can be used to classify HS and LS groups based on previous research.<sup>19-21</sup>

## 2. Material and methods

### 2.1. Participants

Twenty-five HS participants and twenty-five LS individuals were recruited from the general community, by handing out flyers to Nottingham Trent University (NTU) students and placing posters in communal areas across the university campuses. People in specific communities who were thought to meet schizotypy criteria (e.g., those with paranormal beliefs, through paranormal networks) were approached to identify the HS participants. Participants completed an online screening survey on the schizotypy - Schizotypal Personality Questionnaire (SPQ).<sup>7</sup> HS participants scored at least 31 out of 74 on the SPQ and denoted the 90th percentile of schizotypy in the Nottingham population.<sup>27</sup> LS participants scored  $\leq 13$  out of 74 on the SPQ and denoted the 10th percentile of schizotypy in the Nottingham population. Finally, 15 HS participants and 11 LS participants were chosen for the analysis step. Based on the screening survey completed by the participants, they had the following characteristics and personality features: (a) high or low level of schizotypal personality traits, (b) right-handedness, (c) aged between 18 and 45 years, (d) having a close relative (parent, sibling, or partner) with whom they spend more than 10 hours a week in face-to-face or phone contact, and (e) not having a current diagnosis of severe mental disorder, brain injury, neurological disorder, learning disabilities, loss of consciousness for more than five minutes, or a history of alcohol or drug abuse within the last 12 months. Data were collected as part of an emotional

auditory odd-ball task, but we used the post-ERP recording (after the ERP settlement).

Ethical approval for the study was obtained from the School of Social Sciences Research Ethics Committee at Nottingham Trent University (No. 2017/232). Participants provided informed consent before taking part in the study.

### 2.2. EEG recording and preprocessing

Continuous EEG signal was recorded by a 64-channel Biosemi Active-Two Amplifier (Biosemi Inc, Amsterdam, Netherlands) at a sampling rate of 2048 Hz and the international 10/20 electrode setting system was used.

EEG data were preprocessed for removing eye-blink and motion artifacts using EEGLAB toolbox.<sup>28</sup> After down-sampling the data to 256 Hz and re-referencing all channels to the Cz electrode, the data were high-pass filtered with a 1Hz finite impulse response (FIR) filter with zero phase shift. In the next step, the CleanLine EEGLAB plugin was used to remove the 50Hz grid signal to prevent the damaging effect of notch filtering (or even lowpass filtering) on granger causality.<sup>29</sup> EEG data were checked visually to identify and remove artifactual time points, such as muscle and movement-related artifacts. Additionally, an independent component analysis (ICA) was applied to each participant's data to remove the eye movement artifacts.<sup>30</sup> In this step, two HS participants with extreme noisy channels were excluded from further analysis.

After artifact rejection, four-second segments were selected in each trial for the remaining analysis steps. Following that, 16 electrodes (FP1, FP2, F1, F2, F5, F6, C1, C2, C5, C6, P1, P2, P5, P6, O1, O2) were selected in four regions of interest, namely prefrontal/frontal, central, parietal and occipital regions. The topographical placement of these electrodes is shown in Figure 1.

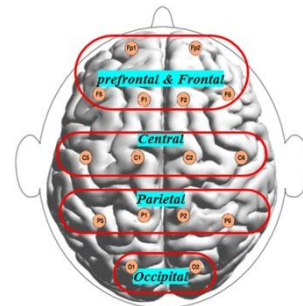


Figure 1. Topographical placement of 16 electrodes subdivided into: prefrontal and frontal electrodes (FP1, FP2, F1, F2, F5, F6), central electrodes (C1, C2, C5, C6), parietal electrodes (P1, P2, P5, P6) and occipital electrodes (O1, O2).

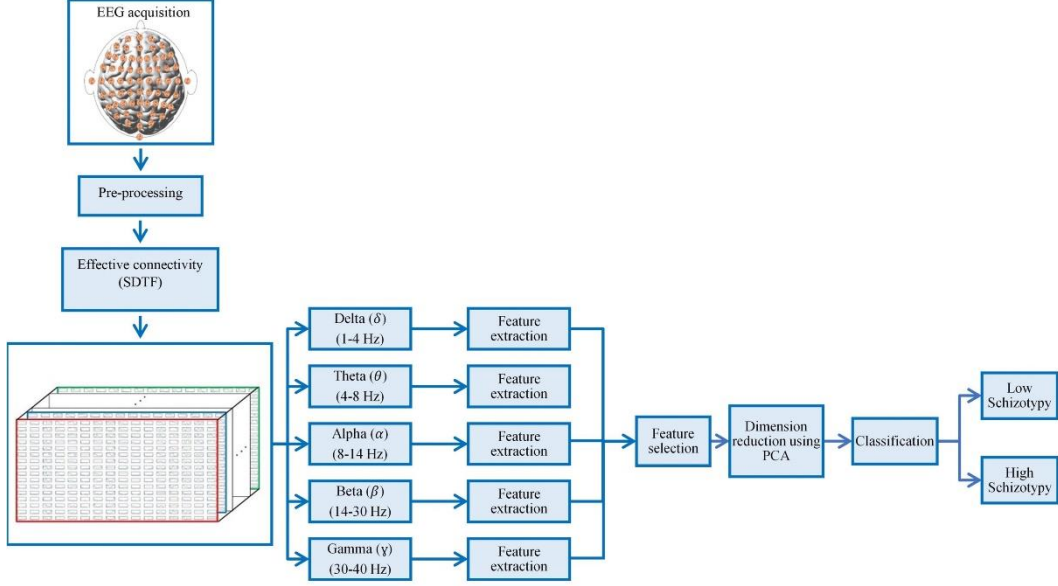


Figure 2. Pipeline of the proposed method. The overall system includes pre-processing, estimation of effective brain connectivity, feature extraction from five conventional brain waves, feature selection, dimension reduction, and classification.

The features have been extracted from each of the five conventional brain waves including delta (1–4 Hz), theta (4–8 Hz), alpha (8–14 Hz), beta (14–30 Hz), and gamma (30–40 Hz), after estimation of effective brain connectivity. Then, a filtering technique has been applied to select a subset of features. After the dimension reduction using principal component analysis (PCA), some popular classifiers have been used to evaluate the schizotypy diagnosis system. Figure 2 illustrates the analysis pipeline of the proposed method.

### 2.3. Estimation of brain connectivity

Some model-based techniques have been developed to obtain the direction of information flow between electrodes. Granger causality (G-Causality) based on the AR model was first introduced by British Econometrician Granger for econometric models<sup>31</sup>, but was afterwards used in the neuroscience and neuroimaging fields<sup>32-34</sup>. G-Causality suggests a brain connectivity measure for calculating the causal interaction of one channel to another (only between two-time series).

For this purpose, MVAR models are employed for estimating the interactions between the paired electrodes in the multichannel EEG data. Univariate AR and its extension MVAR are well-established methods in

prediction and evaluation of system dynamical responses. MVAR model is defined as<sup>35</sup>:

$$\begin{pmatrix} x_1(n) \\ \vdots \\ x_L(n) \end{pmatrix} = \sum_{j=1}^P \begin{pmatrix} A_{11}(j) & \cdots & A_{1L}(j) \\ \vdots & \ddots & \vdots \\ A_{L1}(j) & \cdots & A_{LL}(j) \end{pmatrix} \begin{pmatrix} x_1(n-i) \\ \vdots \\ x_L(n-i) \end{pmatrix} + \begin{pmatrix} e_1(n) \\ \vdots \\ e_L(n) \end{pmatrix} \quad (1)$$

where  $[x_1(n), x_2(n), \dots, x_L(n)]$  is the  $L$ -dimensional time series at time  $n$ ,  $x(n-i)$  is the  $i$ th previous value of  $x(n)$ .

The MVAR coefficients  $A(j) = \begin{pmatrix} A_{11}(j) & \cdots & A_{1L}(j) \\ \vdots & \ddots & \vdots \\ A_{L1}(j) & \cdots & A_{LL}(j) \end{pmatrix}$  form a tensor of size  $L \times L \times P$  and  $[e_1(n), e_2(n), \dots, e_L(n)]$  is the vector of zero mean noise.

$L$  denotes the number of channels and  $P$  is the order of the model that can be obtained using various criteria. The Akaike information criterion (AIC) has been used widely for selecting the best model order. Eq. (1) can be rewritten as follows where  $A(0)$  is an identity matrix:

$$\begin{pmatrix} e_1(n) \\ \vdots \\ e_L(n) \end{pmatrix} = -\sum_{j=0}^P \begin{pmatrix} A_{11}(j) & \cdots & A_{1L}(j) \\ \vdots & \ddots & \vdots \\ A_{L1}(j) & \cdots & A_{LL}(j) \end{pmatrix} \begin{pmatrix} x_1(n-i) \\ \vdots \\ x_L(n-i) \end{pmatrix} \quad (2)$$

After converting Eq. (1) to spectral domain by Z-transform, Eq. (2) is converted to:

$$E(\omega) = A(\omega) X(\omega) \quad (3)$$

where

$$A(\omega) = \sum_{j=0}^P A(j) Z^{-j} \Big|_{z=e^{-i\omega}} \quad (4)$$

and a similar operation is used for calculation of  $X(\omega)$ .

The transfer matrix of the MVAR model for obtaining the causal relationship between channel pairs can be expressed as:

$$H(\omega) = A^{-1}(\omega) \quad (5)$$

The non-normalized DTF between channel  $m$  and channel  $n$  is calculated as follows<sup>13</sup>:

$$\theta_{mn}^2(\omega) = |H_{mn}(\omega)|^2 \quad (6)$$

In this study, the normalized DTF of information flow from  $m$  to  $n$  is computed as (to keep diagonal elements 1):

$$DTF_{m \rightarrow n} = \frac{|H_{nm}(\omega)|}{\sqrt{|H_{nn}(\omega)| * |H_{mm}(\omega)|}} \quad (7)$$

## 2.4. Schizotypy classification

### 2.4.1. Feature extraction

To overcome the nonstationarity problem of EEG signals, short-time DTF (SDTF) method has been suggested<sup>36</sup>. In this study, each signal segment is divided into smaller overlapping segments by sliding a Hamming window over the signal, and MVAR model coefficients  $A(j)$  are estimated by applying a stepwise least squares algorithm to each segment of our multichannel EEG. ARfit Matlab package has been used for this purpose.<sup>37</sup> Following this method, the SDTF or causality relation of channel pairs is obtained using the calculated  $A(j)$  in each window. We define a window size of 1s with a step size of 40ms. Figure 3 provides a graphical representation of this algorithm. The outcome of this algorithm is a 3-D matrix that contains the information flow between pairs of EEG channels in each plane.

To test the consistency of this method, the area under SDTF of the channel pairs for each five frequency bands is calculated as a measure of causality relation strength between the channels and plotted as a function of time. More explicitly, to derive each row in Figure 4, as shown in Figure 3, we first calculate the power, as the area under the DTF curve in each window. The calculated power for the first window is the first value in each row in Figure 4. To derive the subsequent points that construct the whole line, we slide the window over the signals with the aforementioned overlap and repeat the whole procedure. Figure 4 illustrates how acceptably consistent the variation of DTF-based brain connectivity over a short

period for some bilateral channels is. The presence of some fluctuations is due to the nonstationary nature of EEG brain signals. To evaluate the DTF as a measure of effective brain connectivity in different frequency bands, the power was extracted from each five EEG conventional frequency bands i.e., delta (1–4 Hz), theta (4–8 Hz), alpha (8–14 Hz), beta (14–30 Hz) and gamma (30–40 Hz).

### 2.4.2. Feature selection

Selection of independent and influential features is crucial in any classification method. Feature selection is generally used for two purposes: (1) to increase the accuracy of the classification (performance) by reducing the dimensions of the feature space and reducing its complexity, and (2) to select significant and informative features for further steps in the machine learning algorithm.<sup>38</sup> Generally, this technique obtains the optimal number of features and generalized classification results. Various methods have been introduced for this purpose in the literature, such as filtering and wrapper techniques.<sup>39</sup> In this study, the filter technique (t-test) was applied to select the subset of features. The benefits of the filtering technique are the independence of the classifier type and its fast computing. Therefore, extracted features from the five standard frequency bands in the previous step are ranked using a t-test to find which of them has a significant difference between schizotypy groups.

### 2.4.3. Dimensionality reduction

Principal component analysis (PCA) is a common method in feature dimensionality reduction and is widely used in the literature.<sup>40-42</sup> Using an orthogonal conversion, PCA projects the set of possibly correlated variables into the set of linearly uncorrelated variables which are called principal components. To overcome the problem of variable scale and outlier issue in the feature space, the obtained features from the previous level are standardized (z-score normalization) before using PCA.<sup>43</sup> The standard deviation and mean of each feature are determined. Thus, the z-score is calculated as:

$$z = \frac{x - \mu}{\sigma} \quad (8)$$

where  $\mu$  and  $\sigma$  are the mean and standard deviation of each feature, respectively. Hence, obtained feature space provides more accurate and straightforward classifiers in the machine learning algorithm stage.

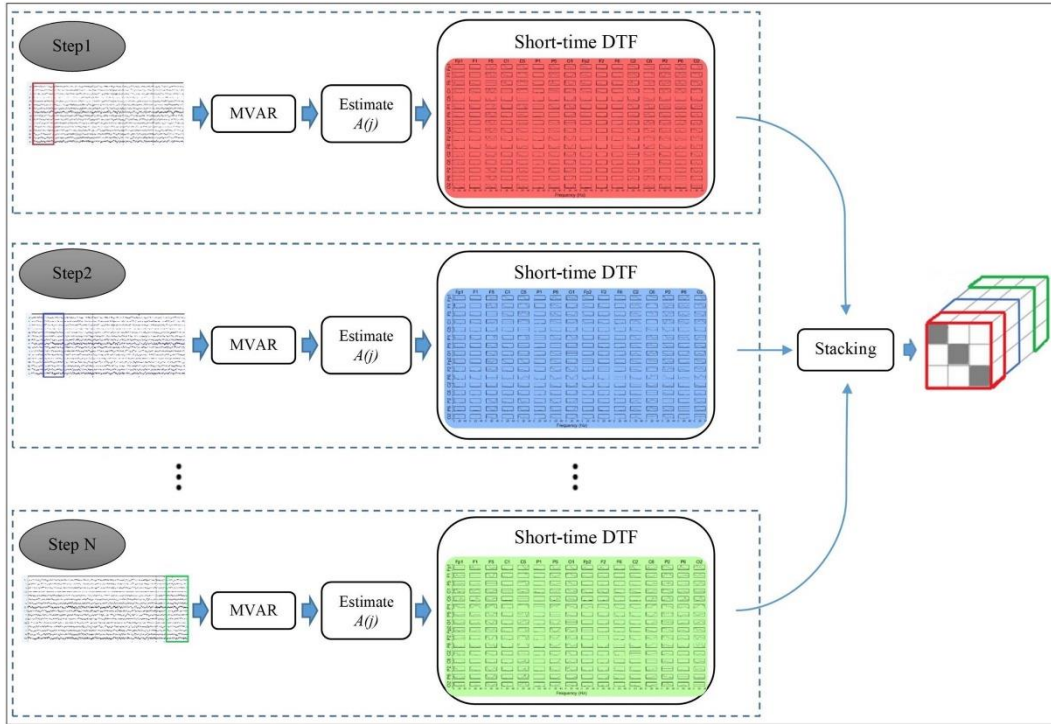


Figure 3. Graphical representation of the proposed method.

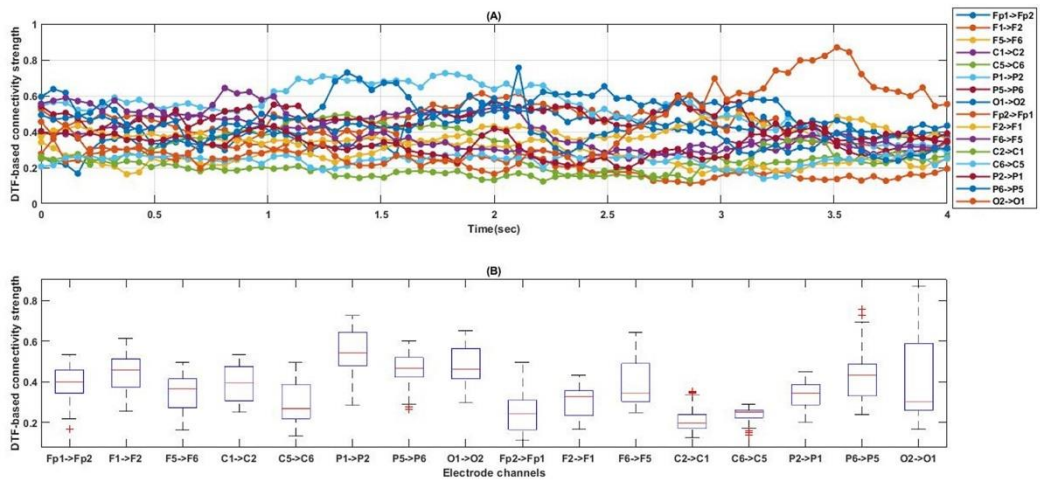


Figure 4. Variation of power causality relation between channels measured by SDTF as a function of time. (A) Fluctuations of the power as a function of time and (B) The oscillation using the box plot.

#### 2.4.4. Classification

After providing the most significant features, some classifiers have been used to distinguish between two (or more) groups (such as HS and LS) using training data sets. In this study, three types of popular classifiers have

been used, namely, linear discriminant analysis (LDA), support vector machines (SVM), and k-nearest neighbor (KNN). LDA is often used in places where the data distribution is approximated as Gaussian. This method distinguishes two linearly separable classes by

constructing a plane or hyperplane in the feature space. Likewise, SVM defines a hyperplane in feature space and finds the best solution to separate two classes by maximizing the margin distance between the nearest feature in each class and the hyperplane. In addition, by definition, the kernel function SVM can be used in two-class problems where the features are not linearly separable.<sup>44,45</sup> In this study, in addition to the linear decision boundary, the radial basis function (RBF) kernel is used to construct the non-linear boundary and reach better accuracy. The kernel function is defined as<sup>13</sup>:

$$K(x_i, x_j) = \exp\left(\frac{-\|x_i - x_j\|^2}{2\sigma^2}\right) \quad (9)$$

where  $\sigma$  is a free parameter that is understood as a cut off parameter for the Gaussian sphere. In this study the Kernel parameters of SVM-RBF have been tuned using a grid search approach ( $C=100$ ,  $\gamma=0.001$ ). This approach is a simple way to tune the hyperparameter used to optimize  $C$  (which controls the model overfitting) and  $\gamma$  (degree of model nonlinearity) parameters in SVM-RBF. A subset of hyperparameter space has been determined using exhaustive grid search manually.<sup>46</sup>

KNN is another popular classifier used in places where the features that are related to each class are relatively close to each other in the feature space. In this algorithm, the metric distances are compared between the test data and the training datasets in the feature space, and then the decision is made by a majority vote based on its  $k$  nearest neighbors.<sup>47</sup>

#### 2.4.5. Validation

To validate the classifier and overcome the leakage between the training and testing procedures, leave-one-subject-out cross-validation (LOSO-CV) is used for performance evaluation.<sup>48</sup> In this procedure, one subject

is used for the test set, and the remaining subjects are used for the training set. Then, the classification accuracy is obtained using the test dataset. Figure 5 illustrates the steps of this method.

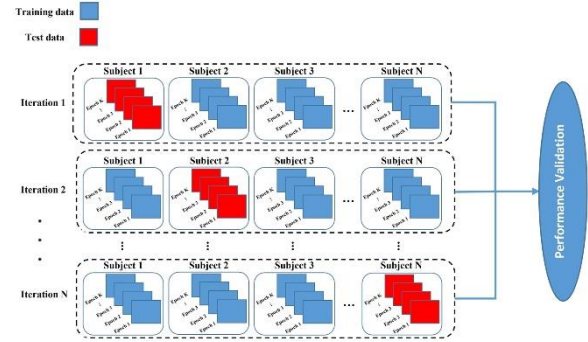


Figure 5. Representation of the LOSO-CV method. In each iteration, a classifier is trained using a training set (blue) and then tested using the test set (red) to obtain the necessary accuracy. The number of iterations is equal to the number of subjects.

In addition, feature extraction and other steps are applied separately to the training and testing sets. In the training process, the label of optimal features and eigenvector of the PCA algorithm are stored for the feature selection and dimensionality reduction in the testing process. The flowchart of the training and testing processes in the proposed method is shown in Figure 6.

Accuracy, specificity, sensitivity, positive predictive value (PPV or precision), and negative predictive value (NPV) are used here to assess the performance. All of these measures are evaluated based on a confusion matrix that contains true positive (TP), false positive (FP), true negative (TN), and false negative (FN). The derivation of the above measures from a confusion matrix is summarized in Table 1.

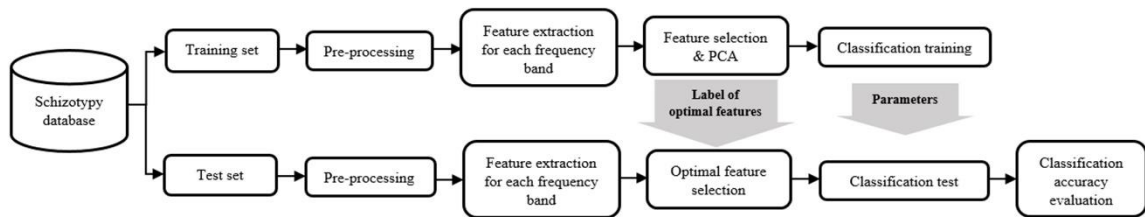


Figure 6. Flowchart of training and testing processes applied to schizotypy classification.

By considering HS and LS classes, each term in the confusion matrix is defined as follow:

TP: the number of correctly identified as HS.

TN: the number of correctly identified as LS.

FP: the number of incorrectly recognized as HS. (belonging to the LS group)

FN: the number of incorrectly recognized as LS. (belonging to the HS group)

Table 1. The derivation of above measures from a confusion matrix.

Measures	Formula
Accuracy	$Acc = \frac{TP + TN}{TP + TN + FP + FN} \times 100$
Specificity	$Spec = \frac{TN}{TN + FP} \times 100$
Sensitivity	$Sens = \frac{TP}{TP + FN} \times 100$
Positive PV	$PPV = \frac{TP}{TP + FP} \times 100$
Negative PV	$NPV = \frac{TN}{TN + FN} \times 100$

### 3. Results

This study is performed by using MATLAB 2019a software on a Windows PC with a 2.27 GHz Intel Core

i5-M430 processor and 8-GB RAM. The average runtime of the classification test step is 0.714s for each subject.

To evaluate the proposed method, twenty-four participants (13 HS and 11 LS) were used. As mentioned earlier, all epochs of one participant were used as a test set, and twenty-three remaining participants (with all epochs) were included in the training set. The whole number of epochs for HS and LS were 928 and 880, respectively. The total number of features was 1200 ([16 electrodes]  $\times$  [16 - 1]  $\times$  5 frequency bands). After ranking the features using t-test, the optimal number of features was determined to be 82. PCA has then been used for dimensionality reduction.

Tables 2 and 3 demonstrate the accuracy of different classifiers for each HS and LS participant, respectively. In addition, the number of epochs for each participant is shown in these tables separately. Table 4 shows the total accuracy (weighted mean) of HS and LS participants for different classifiers.

These results indicate that the classification accuracy for most participants is significantly higher than the chance level. Accordingly, the proposed method can be used as an accurate system to identify HS individuals in the general population. In addition, these results show that the performances of all the classifiers are fairly close to each other and prove the high effectiveness of DTF for this disorder.

Table 2. The accuracy for high schizotypy participants using different classifiers.

Test Data - participant's number	HS-1	HS-2	HS-3	HS-4	HS-5	HS-6	HS-7	HS-8	HS-9	HS-10	HS-11	HS-12	HS-13
Number of Epochs	70	70	70	70	70	70	70	70	62	70	70	96	70
KNN (K=7)	64.3	62.85	95.7	100	81.4	61.4	82.85	94.3	62.9	85.7	85.7	92.7	97.14
LDA	100	65.7	100	100	92.85	87.14	88.6	98.6	75.8	88.6	84.3	100	98.6
Linear SVM	94.3	75.7	100	100	91.4	92.85	82.85	97.14	56.45	98.6	88.6	100	98.6
RBF-SVM	94.3	75.7	100	100	91.4	92.85	82.85	98.6	56.45	98.6	88.6	100	98.6

Table 3. The accuracy for low schizotypy participants using different classifiers.

Test Data - participant's number	LS-1	LS-2	LS-3	LS-4	LS-5	LS-6	LS-7	LS-8	LS-9	LS-10	LS-11
Number of Epochs	80	80	80	80	80	80	80	80	80	80	80
KNN (K=7)	96.25	100.00	78.75	82.50	97.50	83.75	93.75	93.75	52.50	81.25	72.50
LDA	95.00	100.00	76.25	71.25	90.00	86.25	93.75	73.75	41.25	67.50	68.75
Linear SVM	96.25	100.00	87.50	83.75	97.50	91.25	92.50	91.25	41.25	91.25	85.00
RBF-SVM	96.25	100.00	87.50	85.00	97.50	91.25	92.50	91.25	42.50	90.00	85.00

Table 4. The total accuracy [with standard error (SE)] for all participants using different classifiers.

Test Data (Number of Epochs)	HS (928)		LS (880)		ALL (1808)	
	Mean	SE	Mean	SE	Mean	SE
<b>K-NN (K=7)</b>	82.54	0.45	84.77	0.44	83.63	0.31
<b>LDA</b>	91.16	0.33	78.52	0.54	85.01	0.34
<b>Linear SVM</b>	91.05	0.38	87.05	0.51	89.10	0.32
<b>RBF-SVM</b>	<b>91.16</b>	0.38	<b>87.16</b>	0.50	<b>89.21</b>	0.31

A summary of classification performance of the proposed methods is shown in Figure 7. It should be mentioned that this figure is related to the average performance for all of the participants in the LOSO-CV.

To show and evaluate the effect of feature selection and dimension reduction on classification accuracy, Figure 8 compares the accuracy of four classifiers in three modes. However, as can be observed in Figure 8, an evident difference exists between the classification results without feature selection and after the feature selection process.

Figure 9 illustrates the average power of DTF matrices and effective brain connectivity networks in the EEG sensor space for HS and LS groups in each frequency band separately. As can be observed, the connectivity strength has been changed in most frequency bands between the HS and LS groups.

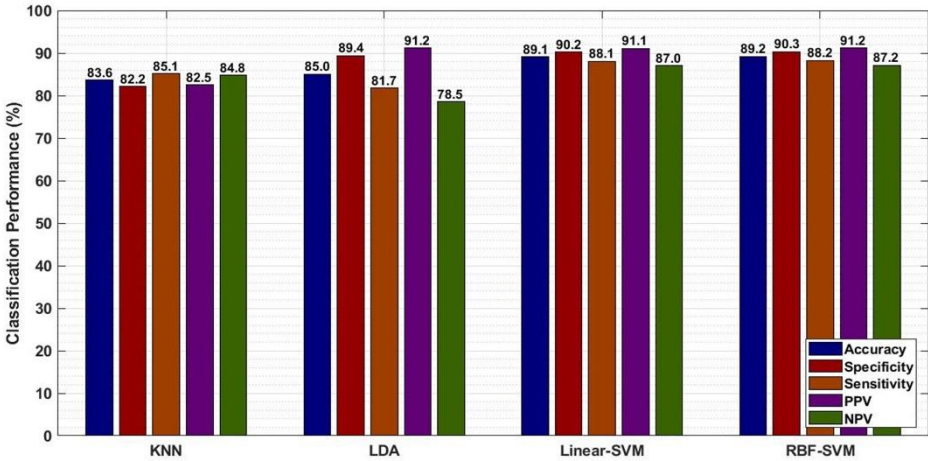


Figure 7. The classification performance. SVM with RBF kernel has the best performance among the four different classifiers.

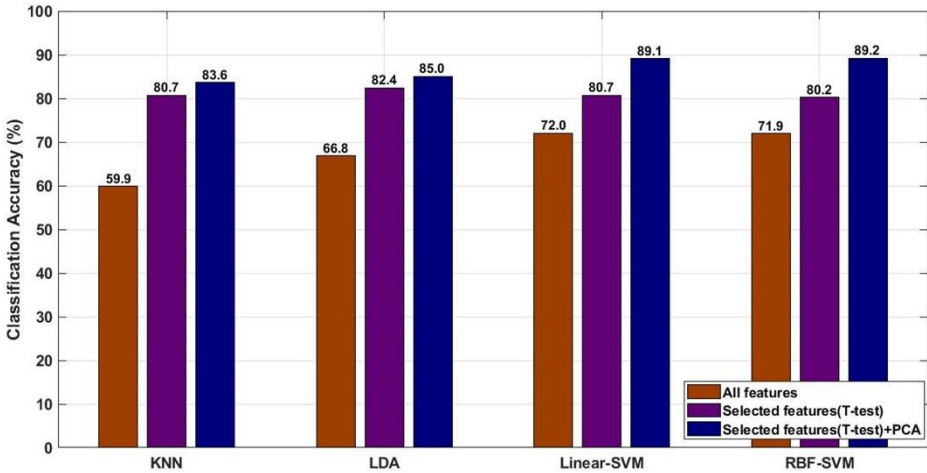


Figure 8. The effect of feature selection and dimension reduction on classification accuracy.

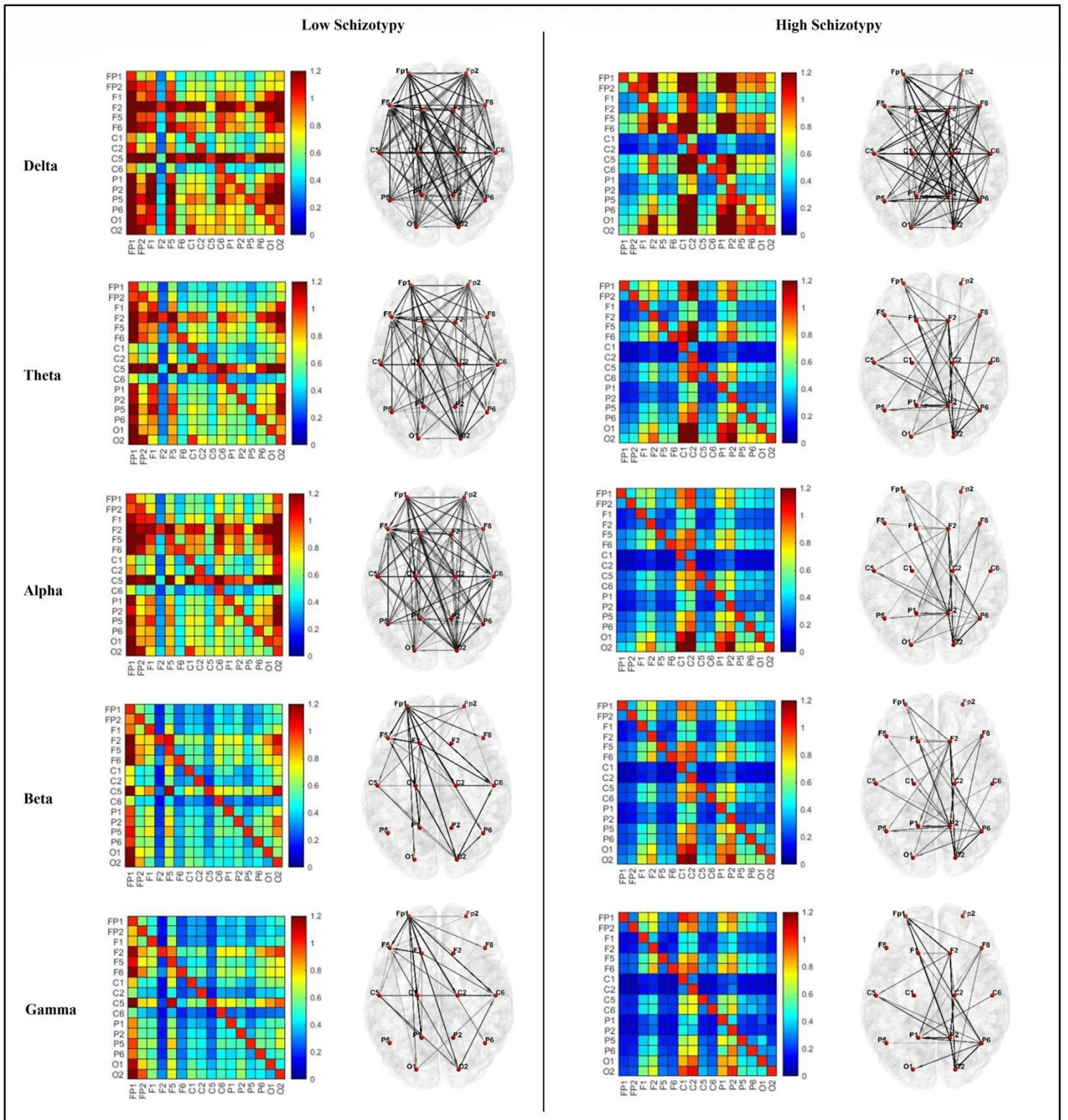


Figure 9. The average power of DTF matrices and effective brain connectivity networks in the EEG sensor space for HS and LS groups in five conventional frequency bands.

Another purpose of this study is to examine the high-rank features in the feature selection step. This process can provide a comparison between the two groups and highlight the significant difference in their effective brain connectivity.

To achieve this goal, the selected features are ranked in each validation step. Then, the filtering technique (t-test) is applied to each training set. Top-ranked features are extracted after sorting them by their p-values in each step. Finally, the seven top-ranked features are selected by considering the union between them in all the steps. It should be mentioned that these seven top-ranked features are present in all the validation processes. The flowchart of the algorithm is shown in Figure 10.

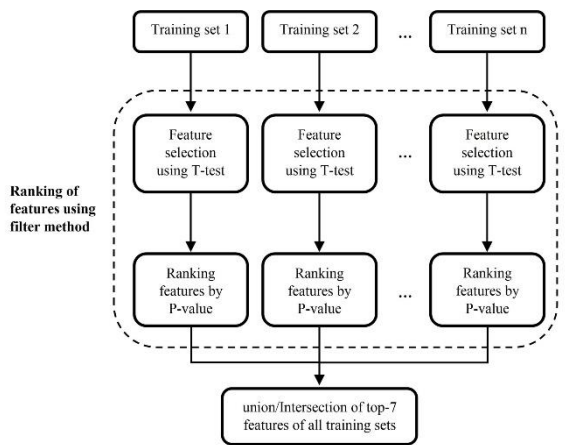


Figure 10. Flowchart of the feature ranking algorithm. The P-value shown in the flowchart results from a t-test between the HS and LS groups.

The comparison of the mean power value of SDTF brain connectivity features between HS and LS participants is represented in Figure 11. Based on Figure 11, a meaningful difference (p-value < 0.001) has been observed between HS and LS groups.

Table 5 shows which frequency bands and channels are related to these seven top-ranked features. As can be observed, most of the top-ranked features belong to the prefrontal/frontal brain regions in  $\alpha$  and  $\beta$  frequency bands. In addition, Figure 12 illustrates the three-dimensional feature space of the principal components for all the participants' epochs after dimensionality reduction using PCA. Evidently, the features of the two classes are clearly separated. Hence, a limited and reliable set of DTFs can form an appropriate classifier for schizotypy diagnosis.

Table 5. The relation between frequency bands and electrode channels in seven top-ranked features.

Rank Number	Channel-pairs (directional)	Frequency band
1	FP2 → FP1	$\beta$
2	FP2 → FP1	$\gamma$
3	F6 → FP1	$\beta$
4	F5 → FP1	$\beta$
5	FP2 → FP1	$\alpha$
6	P6 → FP1	$\beta$
7	F6 → FP1	$\alpha$

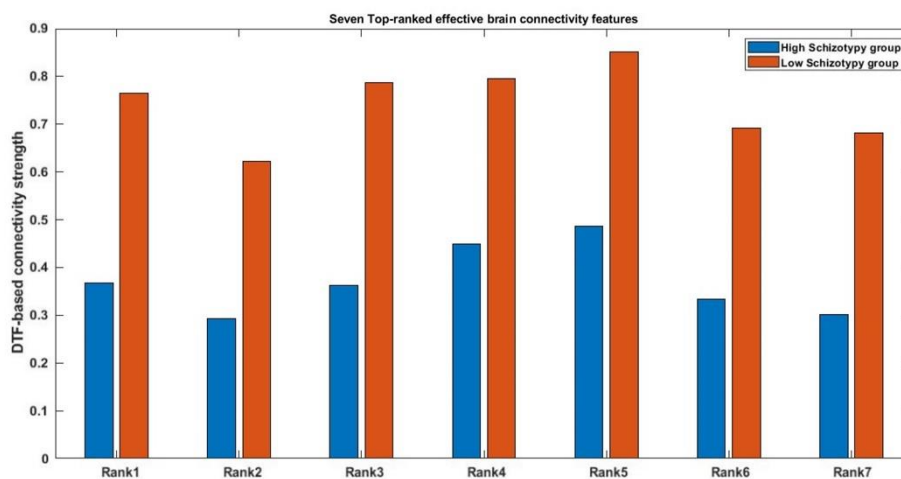


Figure 11. The comparison between seven top-ranked effective brain connectivity features for the two groups.

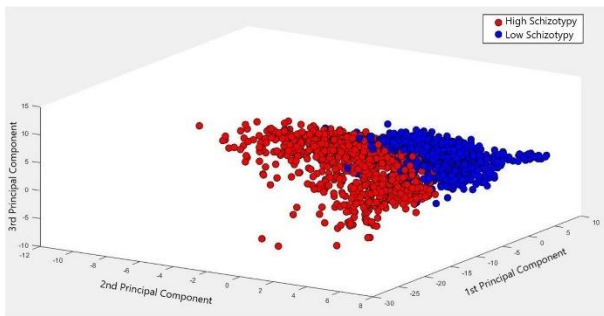


Figure 12. The three-dimensional feature space of the principal components for all the participants' epochs after using PCA.

#### 4. Discussion

The prevalence of severe mental disorders, including schizophrenia, continues to be one of the main problems confronting health care systems.<sup>49</sup> Signal processing and machine learning offer a conducive and efficient system for early diagnosis and monitoring of these disorders.<sup>50</sup> To the best of our knowledge, this study develops the first MVAR-based connectivity measures as reliable features to classify individuals into HS and LS levels. Specifically, we determined the power of DTF derived from MVAR coefficients as features in the separate standard frequency bands between sixteen EEG channels. Our results indicate that the HS and LS participants have significant differences in the  $\alpha$  and  $\beta$  frequency band connectivities. As hypothesised, there was reduced connectivity between prefrontal and parietal regions in the  $\beta$  frequency band. On the other hand, the reduced frontal connectivity in the alpha band in the HS group suggests a diffuse connectivity pattern and low synchrony between brain regions, and possibly poor information flow.<sup>18</sup>

The positive relationship between the schizotypy and schizophrenia patterns has been proved in the first meta-analysis of neuroanatomical mapping of schizotypy.<sup>51</sup> Furthermore, some of the previous studies have found this relation, and argued that schizotypy may lead to schizophrenia and other spectrum disorders.<sup>10,52-55</sup> As per the disconnection hypothesis, the observations of schizophrenia can be generalized to schizotypy.<sup>56</sup> This hypothesis asserts that schizophrenia can be conceived as the faulty interaction of functional systems, such as cortical areas and sub-areas, that are used for adaptive sensory-motor integration, perceptual synthesis, and cognition.<sup>57</sup> Our findings support this hypothesis because the changes in DTF as a measure of effective brain

connectivity are variously associated with HS. The findings indicate that the connectivity pattern in schizotypal individuals can be changed in their connection strengths similar to those of schizophrenics. It is essential to mention that this disconnection syndrome is considered as a function of epigenetic activity and experience-dependent plasticity<sup>57</sup> and indicates effective brain connectivity (not anatomical brain connectivity). Diffuse connectivity patterns have been shown in schizotypy<sup>16-19,58</sup> and schizophrenia patients.<sup>59,60</sup> These phenomena might indicate the deficiency of synchronization between brain regions or the reduction of local computational processing.<sup>59</sup> Furthermore, the resting-state functional connectivity is reduced between frontal and parietal brain regions in HS<sup>19</sup> and first-episode schizophrenia<sup>61</sup> within alpha frequency. Our results have shown that alpha and beta-based effective brain connectivities derived from MVAR are significantly different for the prefrontal/parietal and prefrontal/frontal brain regions. Besides, there is decreased long-distance and short-distance connectivities in alpha and beta bands. Our results are consistent with those of previous studies.<sup>16,19,21</sup> However, in contrast to Ref.<sup>18</sup>, we found a minor difference in occipital connectivity patterns and we observed significant differences in interhemispheric connectivities between HS and LS groups. This divergence of results in between studies may be due not only to differences in data recording and processing methods but also to heterogeneity or inconsistency in detecting psychiatric disorders.<sup>19</sup>

Finally, our results show that effective brain connectivity estimation based on MVAR coefficients may be a reliable criterion for diagnosing the level of schizotypy. Figures 9, 11, and 12 are proof of this assertion. As can be understood from those figures, the features extracted from the DTF are pretty distinct. So, a suitable diagnostic system can be designed based on these features to ensure desirable reliability. Some well-known classifiers were then applied to these features to achieve the best classification rate.

The major limitation of this study is the small sample size. Furthermore, the difference between the two classes is not as high as expected since both groups are from the general (non-clinical) community and not from either perfectly healthy or clinical groups. Generally, schizotypy is a non-clinical form of psychosis-like experiences. So, the level of brain alteration is milder than that in frank psychosis.<sup>9</sup> On the other hand, the cut-

off point for high schizotypy is based on the 90th percentile of a sample of participants in Nottingham City, UK.<sup>27</sup> So, some participants falling on the borderline of high schizotypy might have had a moderate level of schizotypy.

Future studies should consider a larger number of individuals, including clinical and subclinical groups, to obtain a generalization of this study. Future studies should also use more robust and newer classification algorithms (e.g., enhanced probabilistic neural network<sup>62</sup>, neural dynamic classification algorithm<sup>63</sup>, dynamic ensemble learning algorithm<sup>64</sup>, and finite element machine<sup>65</sup>). Our analysis included the sensor-level MVAR based on connectivity measures. In our future studies we will consider more robust methods (e.g., partial directed coherence (PDC) or time reversed Granger causality (TRGC)) to avoid the volume conduction problem<sup>66</sup>, and develop assessment methods based on graph theory to quantify the connectivity networks. We will also involve other measures of brain activity such as variation in frequency bands and most importantly ERPs<sup>67,68</sup> to enhance the robustness of the measurements.

## 5. Conclusions

In this paper we present the first attempt to investigate the identification of schizotypy by estimation of multi-frequency band effective brain connectivity based on MVAR coefficients and use a joint signal processing and machine-learning approach to classify the schizotypy level. This finding indicates significant differences between the prefrontal/parietal and prefrontal/frontal brain regions in alpha and beta frequency bands between HS and LS groups. So, we can reach high classification accuracy using these features. We provide evidence that the effective brain connectivity features could be suitable biomarkers for detection and monitoring of schizotypy and use them for early intervention to prevent some forms of psychosis, including early schizophrenia and spectrum disorders.

## References

1. G. Claridge, C. McCreery, O. Mason, R. Bentall, G. Boyle, P. Slade and D. Popplewell, The factor structure of 'schizotypal' traits: a large replication study, *British Journal of Clinical Psychology*. 35(1) (1996) 103-115.
2. E. H. Thomas, S. L. Rossell, E. J. Tan, E. Neill, T. E. Van Rheenen, S. P. Carruthers, P. J. Sumner, S. Louise, K. Bozaoglu and C. Gurvich, Do schizotypy dimensions reflect the symptoms of schizophrenia?, *Australian & New Zealand Journal of Psychiatry*. 53(3) (2019) 236-247.
3. T. R. Kwapil, K. C. Kemp, A. Mielock, S. H. Sperry, C. A. Chun, G. M. Gross and N. Barrantes-Vidal, Association of multidimensional schizotypy with psychotic-like experiences, affect, and social functioning in daily life: Comparable findings across samples and schizotypy measures, *Journal of abnormal psychology*. 129(5) (2020) 492.
4. T. R. Kwapil and N. Barrantes-Vidal, Schizotypy: Looking Back and Moving Forward, *Schizophrenia Bulletin*. 41(suppl\_2) (2015) 366-373.
5. O. Mason and C. Gordon (eds.) *Schizotypy: new dimensions*, Routledge. 2015.
6. J. Van Os, R. Linscott, I. Myin-Germeys, P. Delespaul and L. Krabbendam, A systematic review and meta-analysis of the psychosis continuum: Evidence for a psychosis proneness-persistence-impairment model of psychotic disorder, *Psychological Medicine*. 39(2) (2009) 179-195.
7. A. Raine, The SPQ: a scale for the assessment of schizotypal personality based on DSM-III-R criteria, *Schizophrenia Bulletin*. 17(4) (1991) 555-564.
8. P. Grant, M. J. Green and O. J. Mason, Models of schizotypy: the importance of conceptual clarity, *Schizophrenia Bulletin*. 44(suppl\_2) (2018) 556-563.
9. U. Ettinger, C. Mohr, D. C. Gooding, A. S. Cohen, A. Rapp, C. Haenschel and S. Park, Cognition and brain function in schizotypy: a selective review, *Schizophrenia bulletin*. 41(suppl\_2) (2015) S417-S426.
10. M.T. Nelson, M.L. Seal, C. Pantelis and L.J. Phillips, Evidence of a dimensional relationship between schizotypy and schizophrenia: A systematic review, *Neuroscience & Biobehavioral Reviews*. 37(3) (2013) 317-327.
11. J. A. Taylor, K. M. Larsen, I. Dzafic and M. I. Garrido, Predicting subclinical psychotic-like experiences on a continuum using machine learning, *NeuroImage*. 241 (2021) 118329.
12. E. Zarogianni, A. J. Storkey, E. C. Johnstone, D. G. Owens and S. M. Lawrie, Improved individualized prediction of schizophrenia in subjects at familial high risk, based on neuroanatomical data, schizotypal and neurocognitive features, *Schizophrenia Research*. 181 (2017) 6-12.
13. S. Sanei and J. A. Chambers, *EEG Signal Processing and Machine Learning*, 2nd Ed, John Wiley & Sons, (2021).
14. U. R. Acharya, V. K. Sudarshan, H. Adeli, J. Santhosh, J. E. Koh and A. Adeli, Computer-aided diagnosis of depression using EEG signals, *European neurology*. 73(5-6) (2015) 329-336.
15. G. Fuggetta, M. A. Bennett, P. A. Duke and A. M. J. Young, Quantitative electroencephalography as a biomarker for proneness toward developing psychosis, *Schizophrenia Research*. 153(1-3) (2014) 68-77.
16. X. Y. Yu, K. R. Liao, Z. K. Niu, K. Wang, E. F. Cheung, X. L. Li and R. C. Chan, Resting frontal EEG asymmetry and schizotypal traits: a test-retest study, *Cognitive Neuropsychiatry*. 25(5) (2020)333-347.
17. T. P. Le, H. D. Lucas, E. K. Schwartz, K. R. Mitchell and A. S. Cohen, Frontal alpha asymmetry in schizotypy: electrophysiological evidence for motivational dysfunction, *Cognitive Neuropsychiatry*. 25(5) (2020) 371-386.

18. D. K. Hu, L. Y. Li, B. A. Lopour and E. A. Martin, Schizotypy dimensions are associated with altered resting state alpha connectivity, *International Journal of Psychophysiology*. 155 (2020) 175-183.
19. J. Trajkovic, F. D. Gregorio, F. Ferri, C. Marzi, S. Diciotti and V. Romei, Resting state alpha oscillatory activity is a valid and reliable marker of schizotypy, *Scientific Reports*. 11(1) (2021) 1-13.
20. L. K. Oestreich, N. G. Mifsud, J. M. Ford, B. J. Roach, D. H. Mathalon and T. J. Whitford, Subnormal sensory attenuation to self-generated speech in schizotypy: electrophysiological evidence for a 'continuum of psychosis'. *International Journal of Psychophysiology*, 97(2) (2015) 131-138.
21. P. Premkumar, M. G. E. Santo, J. Onwumere, M. Schürmann, V. Kumari, S. Blanco, J. Baker and E. Kuipers, Neural responses to criticism and praise vary with schizotypy and perceived emotional support, *International Journal of Psychophysiology*. 145 (2019) 109-118.
22. L. X. Jia, X. J. Qin, J. F. Cui, Q. Zheng, T. X. Yang, Y. Wang and R. C. Chan, An ERP study on proactive and reactive response inhibition in individuals with schizotypy. *Scientific reports*, 11(1) (2021) 1-13.
23. J. W. Jeong, T. W. Wendimagegn, E. Chang, Y. Chun, J. H. Park, H. J. Kim and H. T. Kim, Classifying schizotypy using an audiovisual emotion perception test and scalp electroencephalography. *Frontiers in human neuroscience*, 11 (2017) 450.
24. Q. Chang, M. Liu, Q. Tian, H. Wang, Y. Luo, J. Zhang and C. Wang, EEG-based brain functional connectivity in first-episode schizophrenia patients, ultra-high-risk individuals, and healthy controls during p50 suppression. *Frontiers in human neuroscience*, 13 (2019) 379.
25. W. Klimesch, Alpha-band oscillations, attention, and controlled access to stored information, *Trends in cognitive sciences*. 16(12) (2012) 606-617.
26. L. Wang, X. Li, Y. Zhu, B. Lin, Q. Bo, F. Li, and C. Wang, Discriminative analysis of symptom severity and ultra-high risk of schizophrenia using intrinsic functional connectivity, *International Journal of Neural Systems*. 30(9) (2020) 2050047.
27. A. Castro and R. Pearson, Lateralisation of language and emotion in schizotypal personality: Evidence from dichotic listening, *Personality and individual differences*. 51(6) (2011) 726-731.
28. A. Delorme and S. Makeig, EEGLAB: an open source toolbox for analysis of single-trial EEG dynamics including independent component analysis, *Journal of Neuroscience Methods*. 134(1) (2004) 9-21.
29. L. Barnett and A. K. Seth, Behaviour of Granger causality under filtering: Theoretical invariance and practical application, *Journal of Neuroscience Methods*. 201(2) (2011) 404-419.
30. R. N. Vigário, Extraction of ocular artefacts from EEG using independent component analysis, *Electroencephalography and Clinical Neurophysiology*. 103(3) (1997) 395-404.
31. C. W. J. Granger, Investigating causal relations by econometric models and cross-spectral methods, *Econometrica: Journal of the Econometric Society*. (1969) 424-438.
32. A. K. Seth, A. B. Barrett and L. Barnett, Granger causality analysis in neuroscience and neuroimaging, *Journal of Neuroscience*. 35(8) (2015) 3293-3297.
33. E. Olejarczyk, U. Zuchowicz, A. Wozniak-Kwasniewska, D. Szekely and O. David, The Impact of Repetitive Transcranial Magnetic Stimulation on Functional Connectivity in Major Depressive and Bipolar Disorder Evaluated by Directed Transfer Function and Indices Based on Graph Theory, *International Journal of Neural Systems*. 30(4) (2020) 2050015.
34. Y. Cui, J. Liu, Y. Luo, S. He, Y. Xia, Y. Zhang, D. Yao and D. Guo, Aberrant Connectivity During Pilocarpine-Induced Status Epilepticus, *International Journal of Neural Systems*. 30(5) (2020) 1950029.
35. M. Ortiz, E. Ianez, J. A. Gaxiola-Tirado, D. Gutierrez and J. M. Azorin, Study of the Functional Brain Connectivity and Lower-Limb Motor Imagery Performance After Transcranial Direct Current Stimulation, *International Journal of Neural Systems*. 30(8) (2020) 2050038.
36. M. G. Philiastides and P. Sajda, Causal Influences in the Human Brain During Face Discrimination: A Short-Window Directed Transfer Function Approach, *IEEE Transactions on Biomedical Engineering*. 53(12) (2006) 2602-2605.
37. T. Schneider and A. Neumaier, Algorithm 808: ARfit—A Matlab package for the estimation of parameters and eigenmodes of multivariate autoregressive models, *ACM Transactions on Mathematical Software (TOMS)*. 27(1) (2001) 58-65.
38. U. Raghavendra, U. R. Acharya and H. Adeli, Artificial intelligence techniques for automated diagnosis of neurological disorders. *European neurology*, 82(1-3) (2019) 41-64.
39. Y. Saeys, I. Inza and P. Larrañaga, A review of feature selection techniques in bioinformatics, *Bioinformatics*. 23(19) (2007) 2507-2517.
40. S. Ghosh-Dastidar, H. Adeli and N. Dadmehr, Principal Component Analysis-Enhanced Cosine Radial Basis Function Neural Network for Robust Epilepsy and Seizure Detection, *IEEE Transactions on Biomedical Engineering*. 55(2) (2008) 512-518.
41. M. Graña and M. Silva, Impact of machine learning pipeline choices in Autism prediction from functional connectivity data, *International Journal of Neural Systems*. 31(4) (2021) 2150009.
42. F.J. Martínez-Murcia, A. Ortiz, J.M. Gorris, J. Ramirez, P.J. López-Abarejo, M. Lopez-Zamora and J.L. Luque, EEG Connectivity Analysis Using Denoising Autoencoders for the Detection of Dyslexia, *International Journal of Neural Systems*. 30(7) (2020) 2050037.
43. I. Jolliffe, Principal component analysis, *Encyclopedia of Statistics in Behavioral Science*. (2005).
44. A. Ortiz-Rosario and H. Adeli, Brain-computer interface technologies: from signal to action, *Reviews in the Neurosciences*, 24(5) (2013) 537-552.
45. R. Yuvaraj, M. Murugappan, U. R. Acharya, H. Adeli, N. M. Ibrahim and E. Mesquita, Brain functional connectivity

- patterns for emotional state classification in Parkinson's disease patients without dementia, *Behavioural brain research*. 298 (2016) 248-260.
46. C. W. Hsu and C. J. Lin, A comparison of methods for multiclass support vector machines, *IEEE transactions on Neural Networks*. 13(2) (2002) 415-425.
  47. N. S. Altman, An introduction to kernel and nearest-neighbor nonparametric regression, *The American Statistician*. 46(3) (1992) 175-185.
  48. F. Azarmi, S. N. Miri Ashtiani, A. Shalhaf, H. Behnam and M.R. Daliri, Granger causality analysis in combination with directed network measures for classification of MS patients and healthy controls using task-related fMRI, *Computers in biology and medicine*. 115 (2019) 103495.
  49. J. D. Kropotov, *Functional Neuromarkers for Psychiatry: Applications for Diagnosis and Treatment*, Elsevier Academic Press (2016) 1-462.
  50. H. S. Nogay and H. Adeli, Machine learning (ML) for the diagnosis of autism spectrum disorder (ASD) using brain imaging, *Reviews in the Neurosciences*. 31(8) (2020) 825-841.
  51. M. Kirschner, B. Hodzic-Santor, M. Antoniadis et al., Cortical and subcortical neuroanatomical signatures of schizotypy in 3004 individuals assessed in a worldwide ENIGMA study, *Mol. psychiatry* (2021) 1-10.
  52. E. Bora, Theory of mind and schizotypy: A meta-analysis, *Schizophrenia Research*. 222 (2020) 97-103.
  53. C. Chen, W. Huang, X. Chen, X. Shi, X. Zhu, W. Ma, Y. Wang, Q. Kang, X. Wang, M. Guan and H. Huang, The relationship between resting electroencephalogram oscillatory abnormalities and schizotypal personality traits in the first-degree relatives of schizophrenia patients, *Neuroreport*, 30(17) (2019) 1215-1221.
  54. J-W. Hur, T. Kim, K. IK. Cho and J. S. Kwon, Attenuated Resting-State Functional Anticorrelation between Attention and Executive Control Networks in Schizotypal Personality Disorder, *Journal of Clinical Medicine*. 10(2) (2021) 312.
  55. K. M. Larsen, I. Dzafic, H. Darke, H. Pertile, O. Carter, S. Sundram and M. I. Garrido, Aberrant connectivity in auditory precision encoding in schizophrenia spectrum disorder and across the continuum of psychotic-like experiences, *Schizophrenia Research*, 222 (2020) 185-194.
  56. K. J. Friston, The disconnection hypothesis, *Schizophrenia Research* 30(2) (1998) 115-125.
  57. K. J. Friston, Dysfunctional connectivity in schizophrenia, *World Psychiatry*. 1(2) (2002) 66.
  58. K. H. Madsen, L. G. Krohne, X. Cai, Y. Wang and R. C. Chan, Perspectives on machine learning for classification of schizotypy using fMRI data, *Schizophrenia Bulletin*. 44(suppl\_2) (2018) 480-490.
  59. L. B. Hinkley, S. Vinogradov, A. G. Guggisberg, M. Fisher, A. M. Findlay and S.S. Nagarajan, Clinical symptoms and alpha band resting-state functional connectivity imaging in patients with schizophrenia: implications for novel approaches to treatment, *Biological psychiatry*, 70(12) (2011) 1134-1142.
  60. E. Olejarczyk and W. Jernajczyk, Graph-based analysis of brain connectivity in schizophrenia, *PLoS ONE*. 12(11) (2017) e0188629.
  61. T. Liu, J. Zhang, X. Dong, Z. Li, X. Shi, Y. Tong, R. Yang, J. Wu, C. Wang and T. Yan, Occipital alpha connectivity during resting-state electroencephalography in patients with ultra-high risk for psychosis and schizophrenia, *Frontiers in psychiatry*, 10 (2019) 553.
  62. M. Ahmadlou and H. Adeli, Enhanced probabilistic neural network with local decision circles: A robust classifier, *Integr. Comput.-Aided Eng.* 17(3) (2010) 197-210.
  63. M. H. Rafiei and H. Adeli, A New Neural Dynamic Classification Algorithm, *IEEE Transactions on Neural Networks and Learning Systems*. 28(12) (2017) 3074-3083.
  64. K. M. R. Alam, N. Siddique and H. Adeli, A Dynamic Ensemble Learning Algorithm for Neural Networks, *Neural Computing with Applications*. 32(10) (2020) 8675-8690.
  65. D. R. Pereira, M. A. Piteri, A. N. Souza, J. Papa and H. Adeli, FEMa: A Finite Element Machine for Fast Learning, *Neural Computing and Applications*. 32(10) (2020) 6393-6404.
  66. L. E. Ismail and W. Karwowski, A Graph Theory-Based Modeling of Functional Brain Connectivity Based on EEG: A Systematic Review in the Context of Neuroergonomics, *IEEE Access*. 8 (2020).
  67. M. R. Mannan, K. I. Hiramatsu, H. Hokama and H. Ohta, Abnormalities of auditory event-related potentials in students with schizotypal personality disorder, *Psychiatry and Clinical Neurosciences*. 55(5) (2001) 451-457.
  68. M. A. Niznikiewicz, M. M. Voglmaier, M. E. Shenton, C. C. Dickey, L. J. Seidman, E. Teh, R. Van Rhoads and R. W. McCarley, Lateralized P3 deficit in schizotypal personality disorder, *Biological psychiatry*, 48(7) (2000) 702-705.